
Understanding CNNs from excitations

Zijian Ying

NJUST

zjying@njust.edu.cn

Qianmu Li

NJUST

qianmu@njust.edu.cn

Zhichao Lian

NJUST

lzcts@163.com

Abstract

For instance-level explanation, in order to reveal the relations between high-level semantic information and detailed spatial information, this paper proposes a novel cognitive approach to neural networks, which named PANE. Under the guidance of PANE, a novel saliency map representation method, named IOM, is proposed for CNN-like models. We make the comparison with eight state-of-the-art saliency map representation methods. The experimental results show that IOM far outperforms baselines. The work of this paper may bring a new perspective to understand deep neural networks.

1 Introduction

Instance-level explanation (local explanation) focuses on revealing the impact of different parts of the input example on the output of the model [1]. However, the features as well as high-level semantics extracted by DNNs are usually incomprehensible. Especially in computer vision tasks, the image features extracted by the models are usually abstract. In order to interpret these abstract information, several kinds of methods are proposed, e.g. visualization [6], perturbation [11] and linearization [17]. However, there is a fundamental question of what exactly the signals in a neural networks mean.

Previous works [18, 7] are usually divides the signals into spatial information and high-level semantic information [12]. Then, they use spatial information or high-level semantic information or both information to reveal the operation of the model. And, two questions are generated. The first question is what is the relationship between these two pieces of information? Unfortunately, there is no clear conclusion yet. Another question is human-defined spatial information will make the mapping relationship between output and input inaccurate.

In this paper, with the particularity of instance-level explanations, we attempt to unify the two kinds of information from the perspective of signal excitation and give an explanation of how the two directly interact from a numerical perspective. We name this method PANE (Positive And Negative Excitation). We also show how PANE works on different specific layers and derive the transitivity of excitation. Further more, under the guidance of PANE, we propose a saliency map representation method, named IOM (Input-output mapping). Benifit from PANE, IOM can obtain pixel-level saliency map representation, which means the effect of each pixel and each color channel in the image can be obtained. To the best of our knowledge, this is the first method to convert spatial information and high-level semantic information losslessly. This is also the first pixel-level saliency map representation method.

The overall contributions of our paper are:

1. We provide a novel way to understand neural networks from the perspective of positive signal and negative signal, named PANE. In this sight, all signals can be unified and divided strictly. With the transitivity of excitation, the correlations among output of all layers can be obtained.

2. Under the guidance of PANE, we realize a novel saliency map representation method, named IOM. This method can generate saliency map and analyse the correlation between input instances and features in each dimension.
3. We compare IOM with eight SOTA methods. Experimental results show that IOM significantly outperforms existing competing methods.

2 Positive and Negative Excitation

Let's go back to the bottom of the calculation. The very basic operations in convolution neural networks are addition and multiplication. And the parameters in CNNs, which include input and output of each layer as well as the weights, are usually real numbers. And we all know that real numbers have positive, negative and zero. We call the sign of a real number its explicit property, e.g. 1 is shown as positive. When it comes to a complex signal, what depends the explicit property of the output is the explicit property and absolute value of each input. Here is an example: $1 = 2 + (-1) + 0$. The output 1 is a positive number because it has a positive number 2 and a negative number -1 . The absolute value of 2 is greater than the absolute value of -1 . And zero has no influence on the result. These three things jointly decide the output 1 no matter the sign or the value. If the example becomes: $-1 = -2 + 1 + 0$, these three principles are also fit. Something can be generalized a little. The parts of input signals which have the same explicit property as output has positive excitation. The negative excitation is opposite. Thus, all elements of output signals can be divided into positive excitation, negative excitation and zero (irrelevant) excitation. This can be expressed as:

$$X = X^+ + X^- + X^0$$

where, X is the input signal, X^+ are those input elements which are positive correlated with outcome, X^- are those input elements which are negative correlated with outcome and X^0 are those input elements having no influence on outcome. In order to ease of understanding and for more standardized writing, we give an example here. For two vectors $w \in R^N$ and $v \in R^N$, the inner product is:

$$a = w \cdot v$$

where, a is a real number. We define the sign of a is $Sign(a) \in \{+, -, 0\}$. Expanding the expression on the inner product of vectors, we obtain:

$$a = \sum_{i=1}^N w_i \times v_i = \sum_{i=1}^N Sign(w_i \times v_i) \times |w_i \times v_i|$$

When $a \neq 0$, we can divide all $\{w_i \times v_i, i \in N\}$ into three sets.

$$\begin{aligned} a^+ &= \{w_i \times v_i | Sign(w_i \times v_i) = Sign(a), i \in N\}, \\ a^- &= \{w_i \times v_i | Sign(w_i \times v_i) = -Sign(a), i \in N\}, \\ a^0 &= \{w_i \times v_i | Sign(w_i \times v_i) = 0, i \in N\}. \end{aligned}$$

where, a^+ is the positive excitation which makes a towards the current sign as well as makes the value of a greater, a^- is the negative excitation which makes the value of a smaller, and a^0 is the zero excitation which does not directly influence the a . When $a = 0$, the positive and negative excitation are balanced which means the absolute values of these two parts are equal. In this special case, each of two parts can be either positive excitation or negative excitation.

When we treat vector v as the input signal and a is the outcome, any $\{v_i | \{w_i \times v_i\} \in a^+\}$ belongs to the positive excitation signal a_v^+ which is positive correlated with dominant nature of a . And, w_i is the positive correlation coefficient of v_i . The negative excitation signal a_v^- as well as the zero excitation signal a_v^0 are similar. Each element in input signal belongs to and only belongs to one of these three sets. Thus, we can easily obtain the correlations between input and output.

We name this thought with PANE ((P)positive (A)nd (N)egative (E)xcitation). It is worth noting that, in a broader sense, the specific $\{+\}$, $\{-\}$ and $\{0\}$ change as the domain and operation change. A more approximate analogy is that 0 is similar as the Unitary in Multiplicative Groups. $\{+\}$ and $\{-\}$ are based on the representation of the number field and operation that are greater or smaller relative to 0. In this paper, we only discuss the problem on whole real number field. And, those operations which do not treat real number 0 as 0, e.g. the $\{0\}$ in logarithmic function $\ln(x)$, $x > 0$ is not equal to real number 0, are dismissed. Most of the common layers in CNNs meet the conditions we discussed. We will specially show the derivations in the following section.

3 The Excitation in specific layers

In instance-level explanation, the input signal is fixed. This makes all signals in the entire network a deterministic state. Thus, the input and output of any layer in the network is fixed too. Then, when we study the influence from some parts of input, all other parameters can be treated as known weights. Combining the above and PANE, we will derive excitation signals for some common layers in CNNs individually. We will also discuss how high-level semantic information and spatial information interact with each other.

3.1 Linear layer

Linear layer is usually used as the full connection layer in CNN. Because it is the basic layer in machine learning, we choose to talk this layer first. The expression of a classic linear layer is:

$$Y = w \cdot X + b$$

where, X is the input signal, w is the weight, b is the bias and Y is the output signal. Here we assume $X \in R^M$, $Y \in R^N$, $b \in R^N$ and $w \in R^{N \times M}$. For fixed w and b , the part which is actually correlated with X is $Y' = Y - b$. According to the example listed in the above section, the positive excitation signals of each element in Y' can be obtained. Here, we build excitation matrices to record the corresponding excitation signals of Y' . The each element in positive matrix is represented as:

$$Exc(Y'_X)_{i,j} = \begin{cases} 0, & \text{if } \{w_{i,j} \times X_j\} \notin Y'_i \\ w_{i,j}, & \text{if } \{w_{i,j} \times X_j\} \in Y'_i \end{cases}$$

The specific value of each element in $Exc(Y'_X)$ is the positive coefficient. When the value is equal to zeros, it means that this part of the input signal is not positive correlated with the corresponding output dimension. The negative excitation signal $Exc(Y'_X^-)$ as well as the zero excitation signal $Exc(Y'_X^0)$ has the similar way to be obtained. Since any Y has a fixed influence from bias b , the excitation of Y' actually is also the excitation of Y .

3.2 Convolution layer

The convolutional layer is the most representative and important layer in CNN. The general expression of convolution is:

$$Y = X * f$$

where X is the input signal, f is the convolution kernel and Y is the output signal. In image convolution, this can be defined as $X \in R^{M \times N}$, $f \in R^{m \times n}$ and a stride parameter s , which indicates the sliding step size of the convolution kernel f . Then, the output $Y \in R^{[(M-m)/s]+1 \times [(N-n)/s]+1}$ (shorten with $Y \in R^{o_1 \times o_2}$, where $o_1 = [(M-m)/s] + 1$ and $o_2 = [(N-n)/s] + 1$). This can be rewritten into a linear form.

$$Y^{trans} = X^{trans} \cdot f^{trans}$$

where $Y^{trans} \in R^{(o_1 \cdot o_2)}$, $X^{trans} \in R^{(o_1 \cdot o_2) \times (m \cdot n)}$ and $f^{trans} \in R^{m \cdot n}$. Y^{trans} and f^{trans} are the vector expansion of Y and f . X^{trans} is the complex expansion of X according to f . The relationship of elements in X^{trans} and X is

$$X^{trans}_{i,j} = X_{[i/o_1] \cdot s + [j/m], (i \% o_2) \cdot s + (j \% m)}$$

where, $i \in [0, m-1]$ and $j \in [0, n-1]$. Thus, the original convolution is equivalent to a such linear layer. Then the excitation can be obtained with similar way in linear layer.

We also provide a tensor form of excitation. For any element $Y_{k,l} \in Y$, where $k \in [0, o_1 - 1]$ and $l \in [0, o_2 - 1]$, it is only calculated by the certain slice of X . The process is

$$Y_{k,l} = \sum_{i=0}^{m-1} \sum_{j=0}^{n-1} X_{k \cdot s + i, l \cdot s + j} \cdot f_{i,j}$$

The size of the slice is equal to the size of f . Thus, the excitation of each element in output Y is the corresponding slice from input X . The specific excitation can be obtained, e.g. $Exc(Y'^+) \in R^{o_1 \times o_2 \times m \times n}$. When we explicitly embody the spatial information in the excitation, the corresponding excitation can be expressed as $Exc(Y'_X) \in R^{o_1 \times o_2 \times M \times N}$, where the value of the same place as the slice position is equal and the other places are 0.

3.3 Activation layer

Activation functions filter the input signal and rectify them into a predetermined output distribution. Usually, activation functions are non-linear function. For an instance-level explanation, the correlations between a fixed input signal and the corresponding output can be modeled with a linear mapping. For CNN based networks, we only discuss the *ReLU* activation as an example, whose express is

$$ReLU(x) = \max(x, 0)$$

It is a linear function when $x > 0$. And, it masks those negative values in input signal. Thus, *ReLU* has no negative excitation. The positive excitation signals are the elements whose value is greater than zero. Rest elements belong to the zero excitation. The coefficients of all positive excitation signals are 1.

3.4 Pooling layer

Pooling layer is utilized to expand the receptive field of input signal. Here, we choose Max Pooling and Average Pooling, which are two most common pooling methods, to discuss. The express of Max Pooling is:

$$MaxPool(X) = \max(X)$$

where, $X \in R^{M \times N}$ and $MaxPool(\cdot) \in R$. Max Pooling chooses the maximum value of the area to represent the original entire input signal X . And, Max Pooling, like *ReLU*, only has positive excitation and zero excitation. The only positive excitation of $MaxPool(X)$ is the element $X_{i,j} \in X$ where $X_{i,j} = \max(X)$. The positive coefficient of it is 1.

Average Pooling is much more like the linear layer. The expression is:

$$AveragePool(X) = \bar{X} = \frac{\sum_{i=1,j=1}^{M,N} X_{i,j}}{M \times N}$$

This is the same with a linear function with all weights are $(M \times N)^{-1}$ and the bias is $\mathbf{0}$. The excitation can then be obtained with the sign of input.

3.5 Normalization layer

The essence of normalization is data distribution shifting. For a fixed input signal X , the outcome $Norm(X)$ has a mapping between each corresponding element in X and $Norm(X)$, so that $Norm(X)$ can build a linear mapping to directly obtain X . Here we discuss the Batch Normalization (BN), which is frequently used, as an example. The express is:

$$BN(X) = \frac{X - \mu}{\sqrt{\sigma} + \epsilon} \circ \gamma + \beta$$

where, $X \in R^N$, $\mu \in R$ is the mean value of X , $\sigma \in R$ is the variance of X , ϵ is a small bias to avoid division by zero, \circ is Hadamard product, $\gamma \in R^N$ is a learned weight and $\beta \in R^N$ is the bias for output. To a certain X , μ and σ are fixed. Thereby, they can be treated as a fixed parameter in this static analysis. Then, the expression can be rewritten into a linear function. For any element in outcome $BN(X)$:

$$BN(X)_i = \frac{\gamma_i}{\sqrt{\sigma} + \epsilon} \cdot X_i + \beta_i - \frac{\mu \gamma_i}{\sqrt{\sigma} + \epsilon} = w'_i \cdot X_i + b'_i$$

where, $w'_i = \frac{\gamma_i}{\sqrt{\sigma} + \epsilon}$, $b'_i = \beta_i - \frac{\mu \gamma_i}{\sqrt{\sigma} + \epsilon}$. Then, the excitation of BN layer has a same way to be obtained as the excitation of linear layer.

4 The transitivity of excitation

The input of each layer in the model can be divided into positive, negative and zero excitation according to the different excitations for the corresponding output. Because zero excitation can absorb the input signal to make it have no explicit correlation with corresponding output, the excitation

of zero excitation signal can be filtered. Thus, except the zero excitation, the whole excitation for a N-layer model can be divided into 2^n different excitations.

Meanwhile, we can notice that the positive excitation of positive excitation signals is still the positive excitation. And, the positive excitation of negative excitation signals is still the negative excitation. It's like a sign change in multiplication. Then, the whole 2^n excitation can be categorized into two classes of excitation including positive and negative. Here, we give a two-layer model as an example.

$$Z = \text{ReLU}(w \cdot X + b)$$

This model contains a linear layer and a ReLU activation layer. To obtain the excitation signal of input X for the output Z , the excitation signal Y_X of intermediate variables $Y = w \cdot X + b$ for Z can be firstly obtained according to section 3.1. Then, according to section 3.3, the excitation signal Y_X can be obtained. Finally, the positive excitation signal of any Z_i for input X is

$$\begin{aligned} Z_{X_i}^+ &= Z_{Y_i}^+ \cdot Y_X^+ + Z_{Y_i}^- \cdot Y_X^- \\ Z_{X_i}^- &= Z_{Y_i}^+ \cdot Y_X^- + Z_{Y_i}^- \cdot Y_X^+ \end{aligned}$$

Because ReLU only has positive and zero excitation, $Z_{X_i}^+$ is equal to $Z_{Y_i}^+ \cdot Y_X^+$. When it back to a N-layer model, the positive as well as negative excitation singal of output Z for input X is the sum of 2^{n-1} excitation signal. And the coefficient is the sum of corresponding excitation. Here, we define the general expression of positive and negative excitation. For a N-layer method, X_i is the output signal of the corresponding layer. Especially, X_0 is the original input singal and X_N is the final output. The positive excitation and negative excitation from X_0 to X_N are:

$$\begin{aligned} \text{Exc}(X_{N|X_0}^+) &= \sum \left(\text{Pos} \left(\prod_{i=N}^1 \text{Exc}(X_{i|X_{i-1}}^{\{\cdot\}_i}) \right) \prod_{i=N}^1 \text{Exc}(X_{i|X_{i-1}}^{\{\cdot\}_i}) \right) \\ \text{Exc}(X_{N|X_0}^-) &= \sum \left((1 - \text{Pos} \left(\prod_{i=N}^1 \text{Exc}(X_{i|X_{i-1}}^{\{\cdot\}_i}) \right)) \prod_{i=N}^1 \text{Exc}(X_{i|X_{i-1}}^{\{\cdot\}_i}) \right) \end{aligned}$$

where, $\{\cdot\}_i \in \{+, -\}$, and

$$\text{Pos} \left(\prod_{i=N}^1 \text{Exc}(X_{i|X_{i-1}}^{\{\cdot\}_i}) \right) = \begin{cases} 1, & \text{if sum of } \{\cdot\}_i = \{-\} \text{ is even} \\ 0, & \text{if sum of } \{\cdot\}_i = \{-\} \text{ is odd} \end{cases}$$

5 The interaction of spatial information and high-level semantic information

Changes in spatial information are mainly related to the pooling method. For examples, Max Pooling merely selects the largest value in the receptive field to the represent original slice. Average Pooling utilize the mean value of all element in the receptive field to the represent original slice. These methods of characterizing with only one value makes the spatial information lost. Of cause, because pooling is performed slice by slice, even very small feature maps can still contain inaccurate spatial information corresponding to the original image.

Meanwhile, existing research generally understands the vectorized features extracted from backbone as a point in a high-dimensional space. And, the high-level semantic information is implied in these features. However, from a numerical point of view, each element in the vectorized features is merely selected by transformations in the model. Methods, e.g. flatten and linear layer, can only utilize the value of outcome from these transformations, e.g. Average Pooling as the last layer of backbone.

Combining the above two aspects, it can be obtained that each element of high-dimensional features actually contains corresponding spatial information. From the perspective of PANE, the high-level semantic information and spatial information are the same. For the certain output, the input signal can be decomposed losslessly into three sets. And the sets contain both numerical and spatial information. Thus, each element in high-dimensional features can obtain corresponding and unique spatial information. Also, the spatial information corresponding to the combination of feature elements in the high-dimensional space is also fixed. This is the unification of spatial information and high-level semantic information. CNN itself does not support the lossless interaction of such information, which is why the method of combining high-level semantic information and spatial information at the same time, e.g. Dual Attention Network [3], can effectively improve the performance.

6 Input-Output Mapping

PANE can naturally guide the generation of saliency map. According to content above, we introduce a saliency map representation method to map the input to the output. We name this method IOM. This method contains two step: calculating relative PANE and smoothing.

6.1 Relative PANE

Because all layers are involved into the excitation transmission, Calculating all 2^N subitems of excitations in PANE are very hard. Meanwhile, considering positive excitation is the explicit excitation outcome which means the absolute value is greater than negative excitation, we choose each most representative subitem to represent $Exc(X_{N X_0}^+)$ and $Exc(X_{N X_0}^-)$ respectively. We mark them as relative positive excitation $r\text{-}Exc(X_{N X_0}^+)$ and relative negative excitation $r\text{-}Exc(X_{N X_0}^-)$. The expressions are:

$$r\text{-}Exc(X_{N X_0}^+) = \prod_{i=N}^1 Exc(X_{i X_{i-1}}^+)$$

$$r\text{-}Exc(X_{N X_0}^-) = Exc(X_{N X_{N-1}}^-) \cdot \prod_{i=N-1}^1 Exc(X_{i X_{i-1}}^+)$$

$Exc(X_{i X_{i-1}}^+)$ is more significant than $Exc(X_{i X_{i-1}}^-)$. And, the last negative excitation have a much more directly relation with the output. Thus, we choose all positive excitations as the $r\text{-}Exc(X_{N X_0}^+)$ and the change the last excitation to negative excitation as the $r\text{-}Exc(X_{N X_0}^-)$.

6.2 Smoothing

For each element $X_{N i}$ in X_N , the $r\text{-}Exc(X_{N X_0}^+)_i$ and $Exc(X_{N X_0}^-)_i$ are opposite. When we care why method makes such a decision, $Exc(X_{N X_0}^+)$ may answer the question. And $Exc(X_{N X_0}^-)$ can tell you what restricts the outcome. However, for saliency map representation, $Exc(X_{N X_0}^+)$ is usually enough. In order to get much close to the $Exc(X_{N X_0}^+)$, we apply a simple average smoothing on the $r\text{-}Exc(X_{N X_0}^+)$. For an input $X \in R^{W \times H \times C}$ and the output $Y \in R^N$, the relative positive excitation $r\text{-}Exc(Y_X^+) \in R^{N \times W \times H \times C}$. Thus, for each element $Y_i \in Y$, the corresponding excitation is $r\text{-}Exc(Y_X^+)_i \in R^{W \times H \times C}$. Then it can be smoothed with neighborhood average filtering and normalized into $[-1, 1]$. The saliency map from IOM is

$$IOM(Y_X^+) = \text{Norm}(\text{AcgFlt}(r\text{-}Exc(Y_X^+)_i))$$

where, $\text{Norm}(\cdot)$ is the normalization method, $\text{AcgFlt}(\cdot)$ is the neighborhood average filtering, $IOM(Y_X^+) \in R^{W \times H \times C}$ and each element $IOM(Y_X^+)_w, h, c \in [-1, 1]$.

7 Related Work

To understand what influence the prediction of CNN, previous works tried many ways, such as visualizing the feature map [16, 6] and finding ROI with perturbation [11, 8]. One of very efficient ways is saliency map [13]. Many recent works are focus on the class activation map [18]. [18] changes the structure of CNN and jointly utilize the spatial information and high-level features to obtain the saliency map. [12] makes use of the gradient to obtain the feature map weights. This makes the CAM can directly obtain saliency map without changing the structure of CNN. [2] improves the Grad-CAM with higher derivatives to adjust the position of saliency map. [15] realizes a 'gradient-free' approach. Score-CAM scores the forward propagation of certain classification to obtain the feature map weights. [10] also realizes a 'gradient-free' approach. Ablation-CAM utilizes ablation analysis to determine the importance of each cell on the feature map. Based on sensitivity and conservation, [4] improves Grad-CAM. [9] takes the advantages of the principal components to improve the weights. [5] considers the relationship between global influence and local feature map. Layer-CAM can spatially weight the activations. [14] computes the gradients from biases and makes use of the sum to obtain weights.

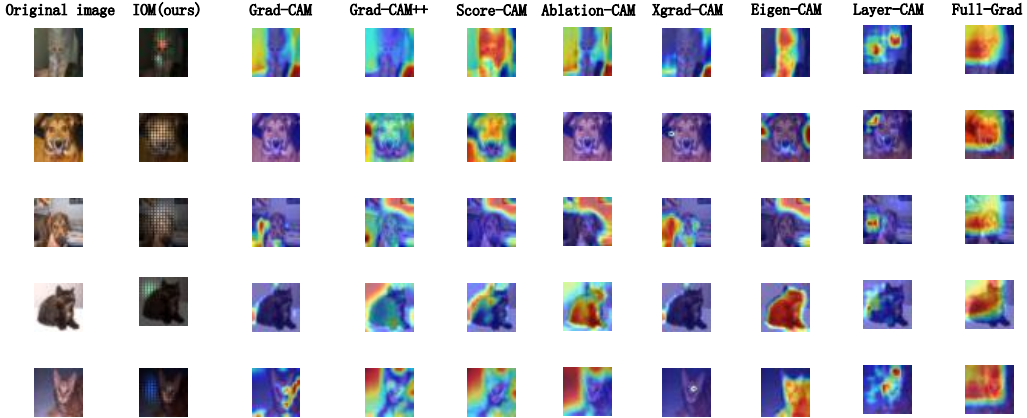


Figure 1: Examples of attention visualization. Images in each row are from a same instance which is under 'Original image'. The attention is generated with corresponding method marked above it. IOM is our method and others are baselines. Red parts of attention from baselines represent high importance area. Blue is just the opposite. Different from baselines, attention from IOM is pixel-level. The highlight area with corresponding color indicates that corresponding color channel of this area has great influence on the result.

8 Experiment

To verify the performance of IOM, we compare IOM with 8 saliency map representation methods. Because there is no code framework that can directly support PANE, we implement a CNN with 6 convolutional layers based on pytorch, and make simple modifications to the bottom layer to meet the basic conditions of PANE operation. These modifications will not affect the normal operation of the CNN. Also, they don't affect baselines. The details of the model is in Appendix. We trained our model on two datasets Dogs vs. Cats and CIFAR10, respectively.

8.1 Baselines

We choose 8 state-of-the-art saliency map representation method to make the comparison. They are Grad-CAM [12], Grad-CAM++ [2], Score-CAM [15], Ablation-CAM [10], XGrad-CAM [4], Eigen-CAM [9], Layer-CAM [5] and Full-Grad [14]. To make sure that all method can work well, we set target layer as the penultimate convolutional layer. This makes sure that the size of feature map is greater than 1. Thus, all baselines can be close enough to the output and have enough spatial information as the same time.

8.2 Visualization and perturbation examples

In order to reduce the negative impact of the number of categories, we visualize IOM with eight baselines on Dogs vs Cats datasets. We directly utilize the absolute value of saliency map generated from IOM and visual the heatmap on the original image. Examples are shown in Fig.1. From these examples, it can be observed that the attention from IOM is more stable then baselines. Many heatmap generated from baselines are far away from the target object, e.g. attention from Grad-CAM++ in the third image. Some methods even fail in some instances such as the heatmap from Grad-CAM in the second image. Meanwhile, we can notice that the heatmap from IOM is closer to the target object, e.g. the attention from IOM in the first image falls in the area of cat and some attention in the fifth image falls in face of the cat.

Something needs to be noticed is the attention from IOM is pixel-level. This means the color of the heatmap not only indicates the importance of area but also indicates the importance of the color channel. If the attention shows a dark blue area, it means the blue channel of these area has a great influence on the result, e.g. the heatmap from IOM in fifth image. And if the attention shows a white area, it means all three channels of this area have a great influence on the result.

Original Image	IOM attention	After perturbation	Prediction(Prob)	Prediction(Vec)
			100% → 99.92%	Ori. [28, 82, 5, 90, 2, 59, -12, 77, -0, 62, -22, 77, -15, 02, -4, 75, 3, 98, 1, 81] Pert. [11, 36, -0, 99, 2, 70, -2, 56, 1, 76, -8, 36, -7, 60, -4, 60, 3, 76, -3, 30]
			100% → 89.45%	Ori. [-2, 47, -11, 46, -1, 08, 22, 22, -8, 75, 7, 94, -3, 72, -3, 18, -1, 74, 1, 55] Pert. [-5, 28, -4, 36, -6, 54, 9, 82, 5, 44, 2, 83, 7, 56, -1, 95, -3, 97, 0, 65]
			99.99% → 20.12%	Ori. [-7, 90, 1, 82, 6, 28, -2, 27, 1, 47, 1, 14, 15, 09, -8, 10, 1, 28, -7, 22] Pert. [-9, 89, -1, 58, 5, 40, 3, 20, 1, 85, 8, 70, 7, 36, -4, 03, -0, 96, -9, 80]

Figure 2: Examples of perturbation. The fist column is the original image. The second column is the attention from IOM. The third column is the image with perturbation. The column ‘Prediction(Prob)’ is the corresponding classification confidence. The last column is output of the classifier. The vector ‘Ori.’ represents the output of original image and the vector ‘Pert.’ represents the output of perturbed image. The bold numbers in vectors are output of corresponding label.

For further verification the effectiveness of IOM, we show some simple perturbation result. If the IOM can work well, the original image X should have a greater corresponding feature value than perturbated image \hat{X} with a simple perturbation from IOM M_X , where $\hat{X} = (1 - M_X) \circ X$. Examples are shown in Fig. 2. We exhibit the change of confidence and output of the Logit layer (last layer of the model) at the same time. It can be obersved that the value of the output has a great reduction with a tiny perturbation. When it comes to the confidence, we can observe that the change of confidence is correlated with all parameter in the output. And, the perturbation and corresponding label are strongly associated. This also verify IOM establishes a clear directivity between the output result and the input signal .

8.3 Comparative Experiment

In order to more objectively evaluate the performance of IOM, we choose the evaluation metric Avgerage Drop% and Win% from [2] as well as the Confidence Drop from [4]. Avgerage Drop% reveals explanation map has dropped how much confidence of the original image. The explanation map here is $E = 0.5 * X + 0.5 * S$, where E is the explanation map, X is the original image and S is the saliency map generated from methods. Win% counts the proportion of the explanation map generated by all methods with the least reduction in confidence. Confidence Drop utilizes the perturbation analysis to observe whether the saliency map is efficient. The perturbated image $\hat{X} = (1 - 1(S')) \circ X$, where $1(\cdot)$ turns all non-zero elements to 1, \circ is Hadamard product. In the saliency map S' , only the pixels greater then mean value of S are set equal to S , while the rest are set to 0. Because IOM is a pixel-level saliency map presentation method, we also count the size of the region affected by the heatmap from all methods and the mean value within the affected region. To make the comparison fairer, we zero out the less than zero portion of the IOM as in the 8 baseline methods. The experimental results are exhibited in the Table 1.

It can be easily observed that effective area of salicency map from IOM is smaller than most baselines. At the same time, IOM’s parameter values are more focused and indicative. Combining these two points to examine the remaining evaluation indicators, it seems not surprised that IOM has a super good performance on Average Drop%. The explanation map from IOM has smaller effective area and lower mean value. However, without heatmap, $0.5 * X$ even has a higher drop than IOM. Not very high value of % Win can also tell us the area and the value is not the matter. Perturbation from explanation map generated by IOM actually has a greater influence on many original images than baselines. When we jointly observe Average Drop % and % Win, we can find that the low value of Average Drop % may caused by more critical locations and effective saliency indications. Because the most area of saliency map generated by IOM are very low value, the mean value of corresponding explanation map is much lower than original image. This might be the reason that IOM does not have a good enough performance on % Win. Confidence Drop also supports this point of view very well. With a very small perturbation area, IOM achieves a good performance. IOM and most baselines perform about the same when the area of perturbation generated by baselines are much larger. This also proves that IOM can well indicate the area where model mainly focuses on.

Table 1: Experimental results of comparative experiments

Methods	Avg. Area%	Avg. Value	Avg. Drop%	% Win	Confi. Drop
No Heatamp	-	-	0.2659	-	-
IOM(our)	0.7245	0.0921	0.2599	0.1145	0.8083
Grad-CAM	0.8847	0.3622	0.4274	0.1048	0.7979
Grad-CAM++	0.9920	0.4353	0.4208	0.0805	0.7898
Score-CAM	0.9898	0.3326	0.3832	0.1096	0.8608
Ablation-CAM	0.9810	0.3944	0.4202	0.0679	0.8277
XGrad-CAM	0.9781	0.3754	0.4250	0.0737	0.8216
Eigen-CAM	0.6761	0.3538	0.4324	0.2065	0.6197
Layer-CAM	0.7656	0.4039	0.4320	0.1086	0.9018
Full-Grad	0.9384	0.4873	0.4388	0.1348	0.9050

9 Conclusion

In this paper, we provide a novel way to understand neural networks from the perspective of positive and negative excitation. From the perspective of PANE, the high-level semantic information and spatial information are unified. Further more, we realize a saliency map representation method IOM to indicate the correlation between specified input signal and output result. To verify the performance of IOM, we make the comparison with 8 baselines. The experimental results shows IOM has very good performance.

References

- [1] Supriyo Chakraborty, Richard Tomsett, Ramya Raghavendra, Daniel Harborne, Moustafa Alzantot, Federico Cerutti, Mani Srivastava, Alun Preece, Simon Julier, Raghuveer M Rao, et al. Interpretability of deep learning models: A survey of results. In *2017 IEEE smartworld, ubiquitous intelligence & computing, advanced & trusted computed, scalable computing & communications, cloud & big data computing, Internet of people and smart city innovation (smartworld/SCALCOM/UIC/ATC/CBDcom/IOP/SCI)*, pages 1–6. IEEE, 2017.
- [2] Aditya Chattopadhyay, Anirban Sarkar, Prantik Howlader, and Vineeth N Balasubramanian. Grad-cam++: Generalized gradient-based visual explanations for deep convolutional networks. In *2018 IEEE winter conference on applications of computer vision (WACV)*, pages 839–847. IEEE, 2018.
- [3] Jun Fu, Jing Liu, Haijie Tian, Yong Li, Yongjun Bao, Zhiwei Fang, and Hanqing Lu. Dual attention network for scene segmentation. In *Proceedings of the IEEE/CVF conference on computer vision and pattern recognition*, pages 3146–3154, 2019.
- [4] Ruigang Fu, Qingyong Hu, Xiaohu Dong, Yulan Guo, Yinghui Gao, and Biao Li. Axiom-based grad-cam: Towards accurate visualization and explanation of cnns. *arXiv preprint arXiv:2008.02312*, 2020.
- [5] Peng-Tao Jiang, Chang-Bin Zhang, Qibin Hou, Ming-Ming Cheng, and Yunchao Wei. Layercam: Exploring hierarchical class activation maps for localization. *IEEE Transactions on Image Processing*, 30:5875–5888, 2021.
- [6] Tsung-Yu Lin and Subhransu Maji. Visualizing and understanding deep texture representations. In *Proceedings of the IEEE conference on computer vision and pattern recognition*, pages 2791–2799, 2016.
- [7] Jiasen Lu, Caiming Xiong, Devi Parikh, and Richard Socher. Knowing when to look: Adaptive attention via a visual sentinel for image captioning. In *Proceedings of the IEEE conference on computer vision and pattern recognition*, pages 375–383, 2017.
- [8] Scott M Lundberg and Su-In Lee. A unified approach to interpreting model predictions. *Advances in neural information processing systems*, 30, 2017.
- [9] Mohammed Bany Muhammad and Mohammed Yeasin. Eigen-cam: Class activation map using principal components. In *2020 International Joint Conference on Neural Networks (IJCNN)*, pages 1–7. IEEE, 2020.
- [10] Harish Guruprasad Ramaswamy et al. Ablation-cam: Visual explanations for deep convolutional network via gradient-free localization. In *Proceedings of the IEEE/CVF Winter Conference on Applications of Computer Vision*, pages 983–991, 2020.

- [11] Marco Tulio Ribeiro, Sameer Singh, and Carlos Guestrin. " why should i trust you?" explaining the predictions of any classifier. In *Proceedings of the 22nd ACM SIGKDD international conference on knowledge discovery and data mining*, pages 1135–1144, 2016.
- [12] Ramprasaath R Selvaraju, Michael Cogswell, Abhishek Das, Ramakrishna Vedantam, Devi Parikh, and Dhruv Batra. Grad-cam: Visual explanations from deep networks via gradient-based localization. In *Proceedings of the IEEE international conference on computer vision*, pages 618–626, 2017.
- [13] Karen Simonyan, Andrea Vedaldi, and Andrew Zisserman. Deep inside convolutional networks: Visualising image classification models and saliency maps. In *In Workshop at International Conference on Learning Representations*. Citeseer, 2014.
- [14] Suraj Srinivas and François Fleuret. Full-gradient representation for neural network visualization. *Advances in neural information processing systems*, 32, 2019.
- [15] Haofan Wang, Zifan Wang, Mengnan Du, Fan Yang, Zijian Zhang, Sirui Ding, Piotr Mardziel, and Xia Hu. Score-cam: Score-weighted visual explanations for convolutional neural networks. In *Proceedings of the IEEE/CVF conference on computer vision and pattern recognition workshops*, pages 24–25, 2020.
- [16] Matthew D Zeiler and Rob Fergus. Visualizing and understanding convolutional networks. In *European conference on computer vision*, pages 818–833. Springer, 2014.
- [17] Quanshi Zhang, Wenguan Wang, and Song-Chun Zhu. Examining cnn representations with respect to dataset bias. In *Proceedings of the AAAI Conference on Artificial Intelligence*, volume 32, 2018.
- [18] Bolei Zhou, Aditya Khosla, Agata Lapedriza, Aude Oliva, and Antonio Torralba. Learning deep features for discriminative localization. In *Proceedings of the IEEE conference on computer vision and pattern recognition*, pages 2921–2929, 2016.